PRAMANA
—journal of
physics



Vol. 48, No. 2,
February 1997
pp. 705–718

# Chaos in jerky flow — Experimental verification of a theoretical prediction

S J NORONHA*, G ANANTHAKRISHNA*, L QUAOUIRE+ and
C FRESSENGEAS+
*Materials Research Centre, Indian Institute of Science, Bangalore 560 012, India
+Laboratoire de Physique et Mécanique des Matériaux, U R A 1215 C N R S, Institut Supérieur de Génie Mécanique et Productique, Université de Metz, Ile du Saulcy, 57045 - Metz Cedex 01, France

**Abstract.** Sometime ago Ananthakrishna and coworkers had predicted the existence of chaos in jerky flow based on a nonlinear dynamical model consisting of the time evolution equations for three types of dislocations and an equation for the evolution of the stress. Our main focus here is to report the verification of this prediction by analysing the stress signals obtained from samples of AlCu alloys subjected to a constant strain rate test. The analysis of the stress signals is carried out by using several methods. The analysis shows the existence of a finite correlation dimension and a positive Lyapunov exponent. We also carry out a surrogate analysis of the time series to ascertain that the signals are not from a power law stochastic process. From the analysis we find that the minimum number of variables required for a dynamical description of the jerky flow appears to be four or five, consistent with the number of degrees of freedom envisaged in the model.

**Keywords.** Jerky flow; Portevin-Le Chatelier effect; dislocations; chaos; correlation dimension; Lyapunov exponent; singular value decomposition; surrogate analysis.

**PACS Nos 05.45; 62.20; 81.40**

## 1. Introduction

The work reported here is an exercise in the application of concepts and techniques in dynamical systems to problems in plasticity. The subject matter falls in the general area of 'stick-slip' phenomenon. For the sake of a general audience, we very briefly recall some basic features of a specific form of plastic instability arising under a constant strain rate test. This is known as jerky flow or the Portevin-Le Chatelier (PLC) effect and has been an object of attention for a long time in metallurgical literature. Dislocations are the basic defects contributing to the plastic deformation of specimens. The stress–strain curves show repeated stress drops and each stress drop in the deformation curve is associated with the occurrence of a dislocation band. The band usually propagates along the sample. The phenomenon is seen in a number of alloys and is known to manifest only in a window of applied strain rates and temperatures [1]. Alloys always contain point defects such as substitutional and interstitial atoms which are commonly referred to as solute atoms. At intermediate temperatures, the cores of these dislocations are saturated with solute atoms, since these atoms have a tendency to migrate

to the cores of the dislocations. Consider a constant strain rate experiment and assume that dislocations are initially free from solute atoms. Once the stress developed in the sample is enough to move dislocations, they sweep the sample and in the process gather solute atoms leading to immobilization of dislocations. This happens once the solute concentration at the core of the dislocation exceeds a certain critical value. However, since the sample is subject to a constant strain rate deformation, the stress in the sample increases to such a value that dislocations break away from the clouds of solute atoms. The breakaway of dislocations results in an yield drop. This whole process repeats thereby multiple yield drops are seen. It is clear that this repetitive nature of the process arises due to a competition of two time scales, namely, the time scale associated with the velocity of dislocations and the diffusion time scale of the solute atoms. This phenomenon is known as dynamic strain ageing (DSA) and was first envisaged by Cottrell [2]. In spite of the enormous attention the subject has received, several aspects of the phenomenon were not well understood until recently. There has been renewed attempts [3–9] to understand this phenomenon by introducing concepts borrowed from the theory of dynamical systems. This has helped to gain new insights hitherto not possible. In most of the models, the negative strain rate sensitivity (SRS) is an input into diffusion like equations [8,9]. Some of these models have been quite successful in explaining a number of features of the PLC effect including the band velocity. Even the existence of chaotic solutions remains a possibility [9]. The first truly dynamical model was attempted by Ananthakrishna and coworkers [3–5] several years ago, wherein the spatial aspect were ignored. This method starts from the time evolution equations for the densities of three types of dislocations. These equations are then coupled to the equation for the stress developed in the sample. The negative SRS results as a consequence of a Hopf bifurcation from a time homogeneous steady state to the time oscillatory state [3–5,12]. The theory has been improved to include the spatial dependence as well [13]. Although, the original theory ignored the spatial aspects, it proved to be surprisingly successful in that it could explain several features of the PLC effect [5,12].

In addition to above results, *one specific prediction of the model is the possibility of chaotic behaviour in a limited range of strain rates* [10, 11]. The first detailed report of the analysis of the experimental stress-strain series which demonstrated the existence of chaos was published recently [14], eventhough, this result was quoted in an earlier paper [13]. Since then there has been a few other investigations which have provided additional support that jerky flow is chaotic [15–17]. *The implication is that the dynamical basis of the model with only a few degrees of freedom is correct* [14].

*The purpose of the paper is to present additional evidence that the dynamics of the underlying phenomenon is indeed chaotic.* The methods include the singular value decomposition, calculation of a finite correlation dimension and a positive Lyapunov exponent. In addition, we carry out surrogate analysis to demonstrate that the time series is not due to a power law stochastic process. The plan of the paper is as follows. In §2, we briefly present the model for the PLC effect which predicts the existence of chaos along with the results related to chaos. In §3, we outline the various methods of analysis used here. We then apply them to the experimental time series. Section 4 contains discussion and conclusions.

## 2. Chaos in a model for the PLC effect

In the following, we very briefly outline our model for the PLC effect [3–5] in terms of scaled variables. Details of the model can be found in the original papers. It is a dynamical model using three types of dislocation densities, namely the mobile dislocation density denoted by $x$, the immobile dislocation density denoted by $y$, and another type which may be regarded as dislocations with clouds of solute atoms denoted by $z$. The basic mechanisms included in the model are: dislocation multiplication through cross glide, annihilation of dislocations, formation of dislocation locks, gradual immobilization of mobile dislocations by solute atoms, and the re-mobilization of the immobile dislocations by stress or thermal activation. These mechanisms lead to a coupled set of nonlinear differential equations for the rate of change of the densities. These rate equations are coupled to the machine equation. Using a power law dependence for the velocity of the mobile dislocations in terms of scaled stress $\phi$ given by $V_m = V_0(\phi)^m$, we can write the equations for the time evolution of dislocation densities and the scaled stress $\phi$ as

$$\dot{x} = \phi^m x - b_0 x^2 - ax + y - xy, \tag{1}$$

$$\dot{y} = b_0[\kappa b_0 x^2 - xy - y + az], \tag{2}$$

$$\dot{z} = c[x - z], \tag{3}$$

$$\dot{\phi} = d[e - \phi^m x], \tag{4}$$

where the parameter $a$ refers to the concentration of the solute atoms, $b_0$ to the strength of reactivation of the immobile dislocations, $c$ to the time scales over which the slowing down of dislocation occurs, $d$ to the effective modulus and $e$ to the applied strain rate. There is a range of values of the parameters $a, b, c, d, \kappa, e$ and $m$ for which we find oscillatory solutions. The model is known to produce a large number of qualitative features of the PLC effect [3–5]. One specific prediction which is of interest here is that the model exhibits chaos in an intermediate range of applied strain rates [10–12]. The model shows the period doubling route to chaos when the velocity exponent $m \geqslant 2$ [11,12]. The value of the Feigenbaum's exponent is the same as that for the quadratic map. For $m > 2$, it shows a bubble structure. For $m$ close to unity, the model shows a period adding phenomenon. Other studies carried out on the model include obtaining approximate closed form expressions for the limit cycles [4] and deriving the time dependent Ginzburg-Landau equation for the order parameter for the creep case [18] (described by equations 1–3). The model has since been extended to include spatial coupling [13]. An additional result that emerges is the velocity of the band.

## 3. Detection of chaotic behaviour in experiments

### 3.1 *Experimental procedure*

Experiments performed under constant strain rate conditions often exhibit two features that are not desirable from the point of dynamical analysis. First, there is an upward drift of the stress-strain curve. The physical origin of this lies in the fact that more and more

dislocations get immobilized and are stored in the sample with a time scale commensurate with the time scale of immobilization. This is called as strain hardening. In addition, there is a gradual increase in the amplitude of the serrations. Clearly both these features are undesirable since they imply nonstationarity of the time series. However, it is often possible to find stress–strain curves which are flat. In the present case, the stress signals are in such a region. The experiments were performed on single crystals of CuAl 14% oriented along $< 111 >$ at 290 K at Poitiers. The strain rate of deformation was $3.34 \times 10^{-4} s^{-1}$. The stress signals were recorded in a digitized form from a single deformation curve. Each set contained 4720 points recorded at a rate of 242 points per second. Even though the data sets are short, we have twelve data sets. As an illustrative example, we will present the results on one data set.

### 3.2 *Time series analysis*

It is known that the stress drops in constant strain rate experiments can appear noisy in a certain regime of the parameter space and devoid of any pattern. Whenever one meets such a noisy sequence, the main objective of any analysis is to determine whether it is of deterministic origin or stochastic origin. In general stochastic noise is always present, for instance, the machine noise or inherent randomness due to other causes.

Our first analysis of the experimental data on Al–Cu alloys [14] has shown that there is a finite correlation dimension. This was obtained using the algorithm due to Grassberger and Procaccia (GP) [19]. However, the existence of a finite correlation dimension cannot always be taken as an indicator of chaotic dynamics. This is because a stochastic process with a power law spectrum can also exhibit a finite correlation dimension [20, 21], and therefore such a process mimics a low dimensional attractor. There are other methods such as singular value decomposition [22] which can be used effectively, particularly when used in conjunction with other methods [23]. Even so, these methods only provide dimensional estimates, and as such cannot always be taken as an evidence of chaotic behaviour. The most reliable quantifier of chaotic dynamics is the existence of a positive Lyapunov exponent. However, conventional methods of determining the Lyapunov exponent require long time series [24, 25] which are impractical to obtain from experiments. Recently, the well known Eckmann's algorithm has been modified to suit short time series [26] giving the entire Lyapunov spectrum. Yet another particularly simple method is due to Gao and Zheng [27]. This method allows one to calculate both the optimum delay time and the optimum embedding dimension in addition to providing an estimate of the positive Lyapunov exponent. Finally, it is always worthwhile to generate surrogate data sets and repeat the analysis to ensure that the signals are not due to a power law stochastic process.

All the methods are based on phase space reconstruction by embedding the signal in a higher dimensional space and carrying out the required analysis. The purpose of embedding a scalar time series in higher dimension is to reconstruct other variables which constitute the dynamics of system from the measured time series. This is done by embedding the signal in higher and higher dimension until an optimum dimension is reached. The object of increasing the embedding dimension is to remove or minimize the contribution from 'false neighbours' since at small embedding dimensions, there are large number of such 'false neighbours'. The rule of thumb for selecting the time lag is to use

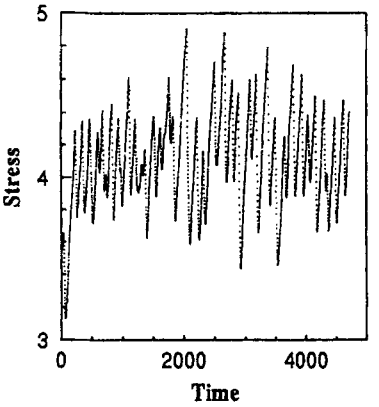


**Figure 1.** A typical stress-time plot for AlCu alloy.

the value of the time at which the correlation function falls to $1/e$ of the initial value. Some use a value of the first zero crossing time. Thus, there is some arbitrariness in estimating the optimal time delay. The method due to Gao and Zheng [27] allows one to determine the optimum value of the time lag as well as the embedding dimension (see below).

Consider a stress signals measured from a jerky flow normally sampled at regular intervals of time represented by $\{\sigma_i = 1, \ldots, N\}$. A typical stress-strain curve is shown in figure 1. The constructed $d$ dimensional vector is $\vec{\xi}_i = \{\sigma_i, \sigma_{(i+\tau)}, \ldots, \sigma_{[i+(d-1)\tau]}\}$, where $\tau$ is some fixed time interval used as a delay. Noise present in the signal can be 'cured' by using singular value decomposition technique. In this method, the (d×N) trajectory matrix $A$

$$A^t = \{\vec{\xi}_1, \vec{\xi}_2, \ldots, \vec{\xi}_N\} \tag{5}$$

is rotated onto the basis of its principal vectors. The $d$ principal values of the matrix $A$ (ie., the eigenvalues of the covariance matrix $A^tA$) are positive. Eigenvalues are conventionally ordered in a decreasing order. If some of the principal values say, $(q+1, \ldots, d)$ are zero, then, it is clear that the trajectory remains confined to the subspace spanned by the basis $(1, \ldots, q)$. In practice the presence of noise prevents these eigenvalues from taking zero value exactly. However, there may be a set of eigenvalues which are small compared to the largest one. Then, an estimate of the embedding dimension is obtained by the sharp decrease in the eigenvalue to a certain low level. It is possible then to obtain the cured trajectory matrix by retaining only the first $q$ components and back rotating these components. Often, this method is used as a noise reduction technique.

The correlation integral $C(r)$ is calculated by

$$C(r) = \frac{1}{N_p} \sum_{i,j} H(r - |\vec{\xi}_i - \vec{\xi}_j|) \tag{6}$$

where $H(\cdot\cdot)$ is the Heaviside step function and $N_p$ is the number of pairs of the embedding vectors $(\vec{\xi}_i, \vec{\xi}_j)$ whose distance is less than $r$. These vectors may refer to either the $d$ dimensional vectors obtained directly from the time series or to the $d$ dimensional vectors

obtained by back rotating the first $p$ principal components. We still need to identify the optimal delay time. This can be done using the following method.

In a chaotic time series, points on two neighbouring trajectories diverge exponentially in time. This divergence can be measured by calculating the distance between them at $t = 0$ and at a later time after $k$ time steps. In a short time the difference vector corresponding to the two points aligns itself in the direction of maximum stretching. Consider two vectors $\vec{\xi}_i$ and $\vec{\xi}_j$ in $d$ dimension. Let $d_{i,j}(k) = \| \vec{\xi}_{i+k} - \vec{\xi}_{j+k} \|$, where $\| \cdot\cdot \|$ is the Euclidean distance between the two vectors at time $k$ between $\vec{\xi}_i$ and $\vec{\xi}_j$. Let $d_{i,j}(0)$ be the initial distance. Since for a chaotic system, $d_{i,j}(k)$ should be larger than $d_{i,j}(0)$, a measure of the divergence is the time dependent Lyapunov exponent $\Lambda(k, d, \tau) = \langle \ln [d_{i,j}(k, z)/d_{i,j}(0)] \rangle$, where $\langle \cdot\cdot \rangle$ refers to the average over all pairs of points for which $d_{i,j}(0)$ is less than a chosen $d_0$. Another quantity is $\Lambda_+(k, d, \tau)$ where the average is limited to those pairs of points for which $(d_{i,j}(k)/d_{i,j}(0)) > 1$. An appropriate window $t_w = (d-1)\tau$ is imposed such that points on the same orbit satisfying $|i - j| > t_w$ are discarded. The optimal time lag is found by looking for the minima in the plots of $\Lambda(\tau, d, k)$ vs $\tau$ and $\Lambda_+(\tau, d, k)$ vs $\tau$ for various values of the embedding dimension. The optimum embedding dimension can also be determined by looking for minimal changes in $\Lambda(\tau, k, d)$ versus $\tau$ as $d$ is increased around the minimum of the curve. In addition, the divergence plots of $\ln [d_{i,j}(k)/d_{i,j}(0)]$ vs $\ln [d_{i,j}(0)]$ do not change much as we increase the embedding dimension beyond a certain dimension which is identified as the optimal embedding dimension.

Since the time series is short, the calculation of the entire Lyapunov spectrum is limited to a few embedding dimensions ($d < 5$). This method is a modification of the algorithm due to Eckmann *et al* [25]. It relies on the construction of a sequence of $(d_M, d_M)$ matrices $T_i$, $(d_M \leqslant d)$ which map the difference vector $\vec{\xi}_i - \vec{\xi}_j$ to $\vec{\xi}_{i+k} - \vec{\xi}_{j+k}$ and successively reorthogonalize $T_i$ using the standard $Q_i R_i$ decomposition. ($Q_i$ is an orthogonal matrix and $R_i$ is an upper triangle matrix with positive diagonal elements.) Then the Lyapunov exponent is given by

$$\lambda_l = \frac{1}{kp\Delta t} \sum_{j=0}^{p-1} \ln(R_j)_{ll}, \quad l = 1, 2, \ldots, d \tag{7}$$

where $p$ is the number of available matrices and $k$ is the propagation time in units of $\Delta t$ which is the time step. The modification effected in this method is to choose all orbits in a shell rather than a sphere so that the effect of randomness is eliminated. The time lag used in this algorithm is the value where the correlation function falls to $1/e$ of the initial value or an optimum choice determined by another method.

Finally, one method of determining if the signals are due to a stochastic process with a power law spectrum is to construct surrogate data sets and repeat the analysis. Surrogate data sets can be generated in a number of ways [21]. One simple way is to take the Fourier transform of the signals randomize their phases and Fourier invert it. If the surrogate data sets do not show a finite correlation dimension or a positive Lyapunov exponent, while the original data sets exhibit both, this is taken as a confirmation that the data is due to a low dimensional attractor.

All the algorithms have been checked against standard benchmark cases such as Rossler and Lorenz attractor; good agreement with the known values in the literature has been obtained.

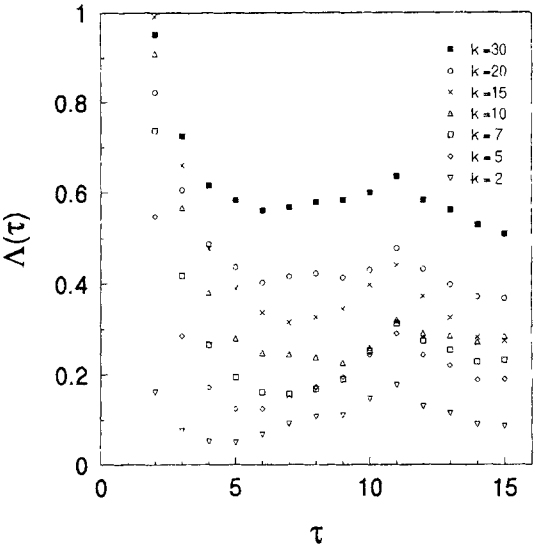


**Figure 2.** A plot of $\Lambda(k,\tau)$ vs $\tau$ for various values of $k$ for the Rossler attractor.

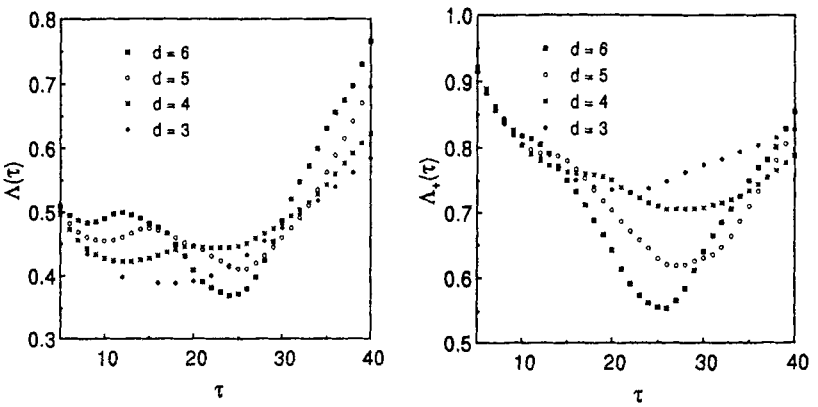


**Figure 3a,b.** A plot of $\Lambda(\tau)$ and $\Lambda_+(\tau)$ vs $\tau$ for $k = 20$ for various values of $d$.

### 3.3 *Analysis of experimental signals*

In the method due to Gao and Zheng, the choice of an appropriate value of $k$ is not specified. Generally, it is so chosen that it reflects a reasonable extent of divergence and is taken to be of the order of the correlation time. However, often one finds that the minima in $\Lambda(\tau,k,d)$ vs $\tau$ coincides with the value of $k$ chosen and therefore gives a spurious optimal lag time. We found that it is possible to estimate the correct value $k$ by plotting $\Lambda(\tau)$ vs $\tau$ for various values of $k$. We find that the minima in $\Lambda(\tau)$ vs $\tau$ for various values of $k$ initially increases as $k$ is increased and then decreases going through a maximum. This maximum value is chosen to be the optimum value of $k$. A plot of $\Lambda(\tau,d,k)$ vs $\tau$ for the Rössler attractor is shown in figure 2 for various values of $k$. The optimum $k$ can be seen to be 9. We find that this value $k_{\text{opt}}$ is independent of the choice of $d_0$.

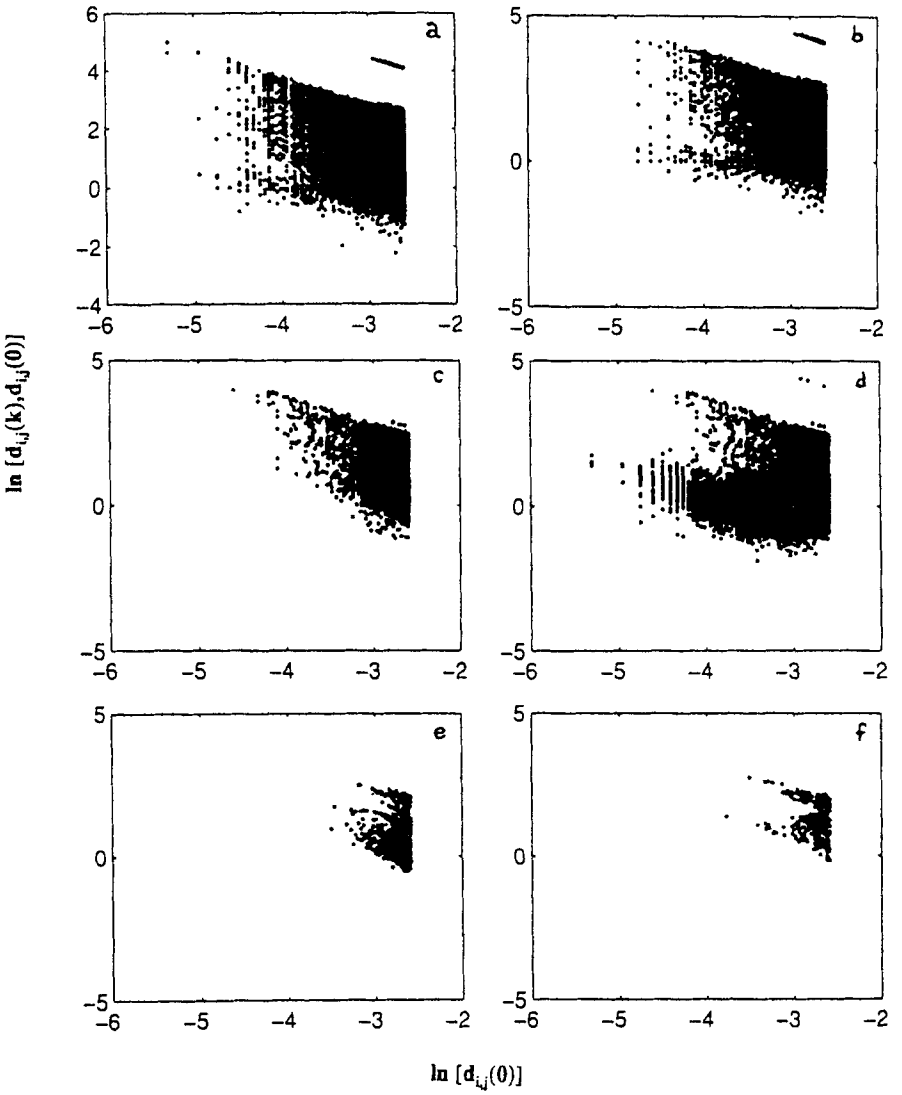


**Figure 4.** The local divergence plots with a window: (**a**) $d = 4, \tau = 27$, (**b**) $d = 5, \tau = 27$, (**c**) $d = 5, \tau = 27$, (**d**) $d = 5, \tau = 27$ (without a window), (**e**) $d = 6, \tau = 27$, (**f**) $d = 6, \tau = 37$.

Figures 3a–b show plots of $\Lambda(\tau, d)$ and $\Lambda_+(\tau, d)$ respectively for $d = 4, 5$ and 6 for $k = 20$ for one data set. When we increase the dimension form 4 to 6, we see that the curve corresponding to $d = 5$ lies lower than $d = 4$, while $d = 6$ does not change significantly from $d = 5$. This suggests that $d = 5$ is the optimum dimension. Further, we also note that the minimum occurs around $\tau = 27$, corresponding to the optimal time lag. Figures 4a–f show the divergence plots for various embedding dimensions and delay times. It is clear that as we approach the optimal $d$, the divergence plots become most compact. Thus, the optimal embedding dimension appears to be $d = 5$. Nonoptimal

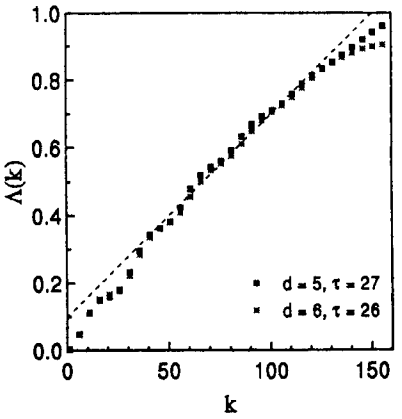


**Figure 5.** A plot of $\Lambda(k)$ vs $k$ corresponding to two different sets of $d$ and $\tau$.

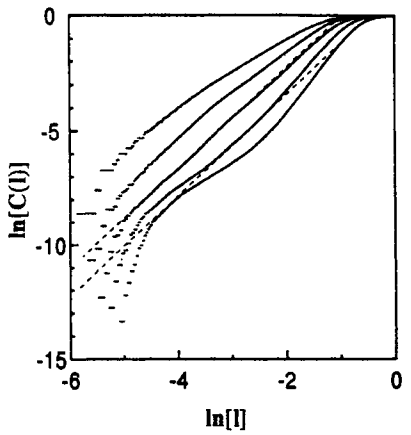


**Figure 6.** Plot of the correlation integral for different $d$ for $\tau_{opt} = 27$.

values of the time lag $\tau$ can be seen to give rise to excess positive excursions over the optimal value. This can be seen from figure 4f shown for $d = 6$ and $\tau = 37$. Note that most of the values are positive even though the plot appears quite compact. Using the value of the optimal time delay, we calculate the time dependent Lyapunov exponent $\Lambda(\tau, k, d)$. This is shown in figure 5 for $d = 5$ and 6. We note that the curve corresponding to $d = 5$ is slightly more linear and has a small positive intercept. The value of the Lyapunov exponent obtained from this plot is 1.4. Having obtained the optimal time delay, we can use this to compute the correlation dimension for this data using the G-P algorithm. This is shown in figure 6. It is clear that even for very small embedding dimension of 5 there is a saturation effect of the slope. Note the dashed straight lines drawn for $d = 4$ and 5 are parallel implying the convergence in the slope. The slope thus obtained is 2.1. It may be worthwhile to point out that the shrinking of the scaling regime starts at fairly small values of $r$ for $d = 6$. Beyond this embedding dimension we find that the scaling regime becomes very small. This behaviour is common to short time series. The saturation of the slope for such a low embedding

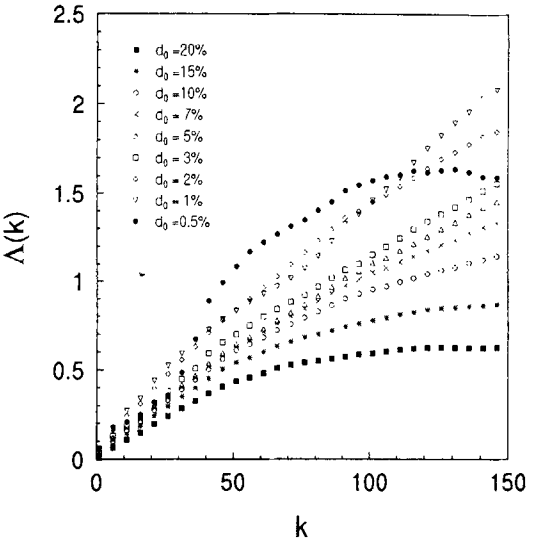


**Figure 7.** A plot of $\Lambda(\tau, k, d)$ vs $k$ for optimum $\tau$ for various values of $d_0$ for the Rossler attractor.

dimension must be contrasted with the high embedding dimension required for a similar saturation in our earlier calculation where a much shorter time lag was employed. This can be clearly attributed to the small delay time that was used in our previous calculation [14] since it is the total window length $t_w$ that remains constant.

It is worthwhile to comment here on the actual values of the Lyapunov exponent obtained by this method. We found that the Lyapunov exponent depends on the value of $d_0$ chosen. Using large values of $d_0$ gives smaller values of the exponent, since the number of points contributing to the average is large, and often, is not a true indicator of the divergence. On the other hand, if too few points are included ( ie., $d_0$ is small) then the statistics gets poor as is the case for $d_0 = 0.05\%$ of the attractor. Indeed, the extent of linearity appears to be less when $d_0$ is large and it improves as $d_0$ is reduced. It appears to break down for small values. Thus a choice of a few percent appears to be reasonable. This is shown in figure 7 for the case of the Rossler attractor. The value of the Lyapunov exponent obtained by this method is a lower bound to that obtained via calculations (which give the largest exponent [24] or the entire spectrum), since in the present method the average is over all possible values including the contracting directions. Even so, we feel that fixing an appropriate value of this parameter in a way that gives a correct value of the Lyapunov exponent for the experimental signals is not easy due to the presence of noise and therefore, the actual value cannot be taken seriously. However, it must be emphasized that the Lyapunov exponent is positive. This is an adequate criterion for the time series to be chaotic.

The singular value decomposition technique has been used to analyse the data as well. The spectrum for various values of window length $t_w$ is shown in figure 8 . It is clear that there is a sharp drop in the relative magnitude of the eigenvalues. Indeed, the maximum fall is at the second component. The changes there after are not so large. This shows that the number of degrees of freedom is of the order of two or three, consistent with the value

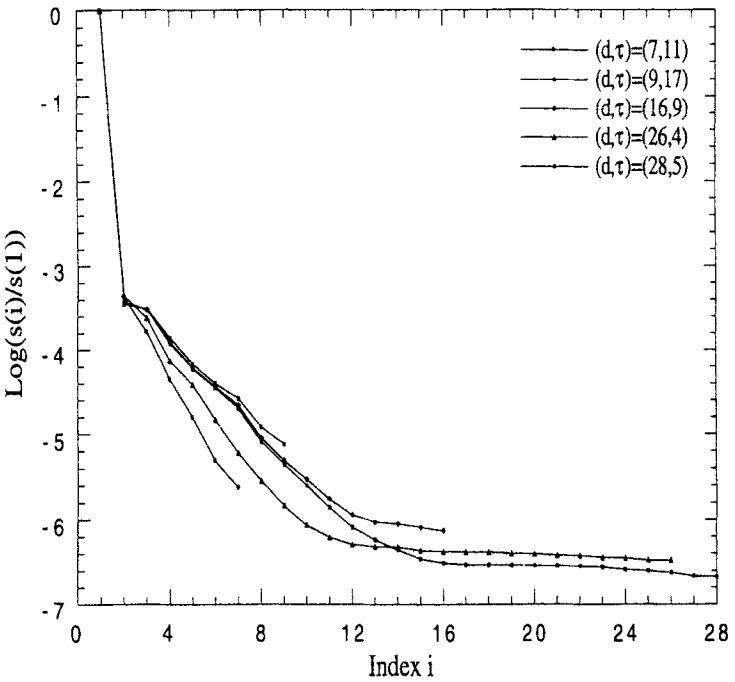


**Figure 8.** A plot of the singular value spectrum for various values of window length.

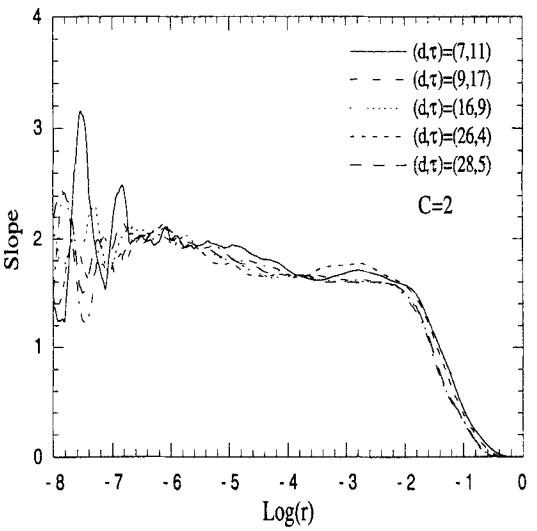


**Figure 9.** A plot of slope of the correlation integral for various values of window length retaining only the first two principal components.

obtained from calculation of the correlation dimension. As an illustration of the method, we can estimate the correlation dimension on the cured time series obtained by back rotating by keeping only the first few components. Figure 9 shows the result obtained by keeping only two components. The convergence of the slope is clearly around 2. General

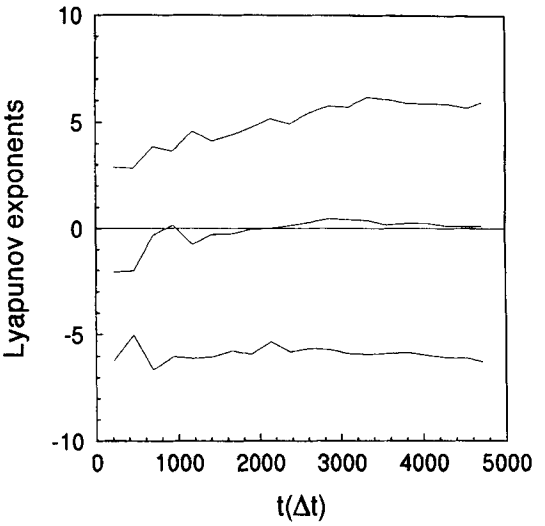


**Figure 10.** A plot of the Lyapunov spectrum as a function of time for $d = 3$ for the original data.

features are not altered if more components are included, since the correlation dimension when all the components are considered is 2.1 as seen from figure 6.

The spectrum of Lyapunov exponents have been calculated using a delay time of $\tau = 27$ for the first few embedding dimensions. From $d = 3$, we find a positive exponent. A plot of the Lyapunov spectrum as a function of time (in units of $\Delta t$ ) is shown for $d = 3$ in figure 10. The value of the largest, the smallest and the zero exponent remains roughly the same from $d = 3$ up to $d = 5$. However, there is an additional positive Lyapunov exponent seen for $d = 5$ which is spurious. This statement is based on calculations carried out on standard models like the Lorenz and the Rossler attractor. In these two cases, we find that at $d = 5$, there is an additional spurious positive eigenvalue. This is due to the fact that we need at least 10000 points for $d = 5$.

Finally, we have generated six surrogate data files. We have calculated both the correlation dimension and the Lyapunov spectrum. We find no saturation in the slope of the scaling regime in any of the six surrogate data sets. Further, we do not see any positive Lyapunov exponent for dimensions up to $d = 5$ for any of the six surrogate files. This clearly shows that the underlying dynamics of the original data is due to a low dimensional attractor.

## 4. Discussion and conclusions

Using a combination of several methods we have analysed time series obtained from experiments on AlCu alloys. The singular value decomposition method clearly shows that the orbit is confined mostly to a few dimensions. We have used a method due to Gao and Zheng to obtain the optimum time delay and the optimum embedding dimension. Since the method gives positive values for the Lyapunov exponent, one can confidently say that the jerky flow is chaotic. In addition, using the optimum value of the time lag, we have

calculated the correlation dimension of value 2.1. We also have calculated the spectrum of Lyapunov exponents by a method suited for short time series. There is one positive Lyapunov exponent of magnitude $\sim 4$. We have further carried out a surrogate analysis to show that the time series is due to a low dimensional chaotic attractor. These calculations confirm the theoretical prediction that jerky flow could be chaotic. Further, the analysis shows the optimum embedding dimension for the time series to be $d_{\text{opt}} = 5$. This is also consistent with the correlation dimension 2.1 obtained by using optimal time delay of $\tau_{\text{opt}} = 26$. *In conclusion, the important prediction, namely, the existence of chaotic flow in the PLC effect is confirmed. This verification strongly suggests the inherent correctness of the basis of the theory, namely, that the dynamical origin of the PLC effect is the nonlinear interaction between the participating defects. Further, the optimum embedding dimension being 5 tells us that we need only five degrees of freedom to describe the dynamics of jerky flow.* We recall that we had only four degrees of freedom since the variable corresponding to the concentration of solute atoms was deliberately suppressed in the original formulation of the model for the sake of simplicity. Lastly, it may be recalled that the phenomenon is spatially inhomogeneous which implies infinite degrees of freedom. Thus, these few degrees of freedom must correspond to the collective behaviour of dislocations and other defects. This fact gives a clue as to why this theory works so well in spite of the fact that it ignores the spatially inhomogeneous aspect which is thought to be so crucial for a proper description of the phenomenon.

## Acknowledgement

This work is partly supported by IFCPAR Grant No. 1108-1. One of the authors (GA) wishes to acknowledge the support from IUFM de Lorraine and the Univeristé of Metz. The authors are thankful to the Poitier's group for supplying the data.

## References

[1] B J Brindley and P J Worthington, *Metal. Rev.* **145**, 101 (1970)
[2] A H Cottrell, *Phil. Mag.* **44**, 829 (1953)
[3] G Ananthakrishna and D Sahoo, *J. Phys.* **D14**, 2091 (1981)
[4] M C Valsakumar and G Ananthakrishna, *J. Phys.* **D16**,1055 (1983)
[5] G Ananthakrishna and M C Valsakumar, *J. Phys.* **D15**, L171 (1982)
[6] L P Kubin and Y Estrin, *Acta Metall.* **33**, 397 (1985)
[7] L P Kubin and Y Estrin, *Acta Metall.* **38**, 697 (1990)
Y Estrin and L P Kubin, *J. Mech. Behavior of Materials* **2**, 255 (1989)
[8] Viewpoint Set on Propagative Instabilities, *Scripta Metall. Mater.* **29**, 1147 (1993)
[9] V Jeanclaude, C Fressengeas and L P Kubin, *Non Linear Phenomena in Materials Science II: Solid State Phenomena*, Vol 23–24, ( Switzerland: Trans Tech Publications 1992) pp. 403.
[10] G Ananthakrishna and M C Valsakumar, *Phys. Lett.* **A95**, 69 (1983)
[11] T M John and G Ananthakrishna in *Directions in Chaos* Ed. Hao Bai-Lin, (Singapore: World Scientific 1990), pp 133
[12] G Ananthakrishna in *Non Linear Phenomena in Materials Science II: Solid State Phenomena*, Vol 23–24, (Switzerland: Trans Tech Publishers 1992) pp. 417
[13] G Ananthakrishna, *Script. Met.* **29**, 1183 (1993)
[14] G Ananthakrishna, C Fressengeas, M Grosbras, J Vergnol, C Engelke, J Plessing, H Neuhäuser, E Bouchaud, J Planés and L P Kubin, *Scripta Metall. Mater.* **32**, 1731 (1995)

[15] G Ananthakrishna and S J Noronha, *Solid State Phenomena*, Vol 42–43, (Switzerland: Scitech Publishers 1995), pp. 277
[16] L Quaouire and C Fressengeas, *Solid State Phenomena*, Vol 42–43, (Switzerland: Scitech Publishers 1995), pp. 293
[17] S Venkadesan, K P N Murthy and M C Valsakumar, *Solid State Phenomena*, Vol 42–43, (Switzerland: Scitech Publishers 1995), pp. 287
[18] M Bekele and G Ananthakrishna, in, *Solid State Phenomena*, Vol. 42–43, (Switzerland: Scitech Publications 1995) pp. 303; M Bekele and G Ananthakrishna, submitted to *Physica D*
[19] P Grassberger and I Procaccia, *Physica* **D9**, 189 (1983)
[20] A R Osborne and A Provenzale, *Physica* **D35**, 357 (1989)
[21] J Theiler, S Eubank, A Longtin, B Galdrikian and J D Former, *Physica* **D58**, 77 (1992)
[22] B S Broomhead and G P King, *Physica* **D20**, 217 (1986)
[23] A M Albano, J Muench, C Schwartz, A I Mees and P E Rapp, *Phys. Rev.* **A38**, 3017 (1988)
[24] A Wolf, J B Swift, H L Swinney and J A Vastano, *Physica* **D16**, 285 (1985)
[25] J P Eckmann, S O Kamphorst, C Ruelle, and S Cileberto, *Phys. Rev.* **E34**, 4971 (1986)
[26] X Zeng, R Eykholt and R A Pielke, *Phys. Rev. Lett.* **66**, 3229 (1991)
[27] J Gao and Z Zheng, *Phys. Rev.* **E49**, 3807 (1994)